HHS Public Access

Author manuscript

Clin Cancer Res. Author manuscript; available in PMC 2014 May 20.

Published in final edited form as:

Clin Cancer Res. 2011 August 15; 17(16): 5367–5378. doi:10.1158/1078-0432.CCR-10-3176.

Targeting Src in Mucinous Ovarian Carcinoma

Koji Matsuo[1,2], **Masato Nishimura**[1,3], **Justin N. Bottsford-Miller**[1], **Jie Huang1**, **Kakajan Komurov**[4], **Guillermo N. Armaiz-Pena**[1], **Mian M. K. Shahzad**[1,5], **Rebecca L. Stone**[1], **Ju Won Roh**[1], **Angela M. Sanguino**[1], **Chunhua Lu**[1], **Dwight D. Im**[6], **Neil B. Rosenshien**[6], **Atsuko Sakakibara**[7], **Tadayoshi Nagano**[7], **Masato Yamasaki**[8], **Takayuki Enomoto**[9], **Tadashi Kimura**[9], **Prahlad T. Ram**[4], **Kathleen M. Schmeler**[1], **Gary E. Gallick**[10], **Kwong K. Wong**[1], **Michael Frumovitz**[1], and **Anil K. Sood**[1,10,11,*]

[1]Department of Gynecologic Oncology and Reproductive Medicine, MD-Anderson Cancer Center, University of Texas, Houston, TX, USA

[2]Department of Obstetrics and Gynecology, Norris Comprehensive Cancer Center, University of Southern California, Los Angeles, CA, USA

[3]Department of Obstetrics and Gynecology, University of Tokushima, Japan

[4]Systems Biology, MD-Anderson Cancer Center, University of Texas, Houston, TX, USA

[5]Department of Obstetrics and Gynecology, University of Wisconsin School of Medicine and Public Health, Madison, WI, USA

[6]The Gynecologic Oncology Center, Mercy Medical Center, Baltimore, MD, USA

[7]Department of Obstetrics and Gynecology, Kitano Hospital, Osaka, Japan

[8]Department of Obstetrics and Gynecology, Osaka Rosai Hospital, Osaka, Japan

[9]Department of Obstetrics and Gynecology, Osaka University Graduate School of Medicine, Osaka, Japan

[10]Cancer Biology, MD-Anderson Cancer Center, University of Texas, Houston, TX, USA

[11]Center for RNA Interference and non-Coding RNA, University of Texas, Houston, TX, USA

Abstract

PURPOSE—Mucinous ovarian carcinomas have a distinct clinical pattern compared to other subtypes of ovarian carcinoma. Here, we evaluated (i) stage-specific clinical significance of mucinous ovarian carcinomas in a large cohort and (ii) the functional role of src kinase in pre-clinical models of mucinous ovarian carcinoma.

EXPERIMENTAL DESIGN—1302 ovarian cancer patients including 122 (9.4%) cases of mucinous carcinoma were evaluated for survival analyses. Biological effects of src kinase

*Address correspondence to: Anil K. Sood, MD, Professor, Departments of Gynecologic Oncology and Cancer Biology, M. D. Anderson Cancer, Center, University of Texas, 1155 Herman Pressler Street, Unit 1362, PO Box 301439, Houston, TX 77230-1439, USA, Phone: +1-713-745-5266, Fax: +1-713-792-7586, asood@mdanderson.org.

Disclosure: There was no conflict of interest for all authors.

inhibition were tested in a novel orthotopic mucinous ovarian cancer model (RMUG-S-ip2) using dasatinib-based therapy.

RESULTS—Patients with advanced-stage mucinous ovarian cancer had significantly worse survival compared to those with serous histology: median overall survival, 1.67 *versus* 3.41 years, p=0.002; and median survival time after recurrence of 0.53 *versus* 1.66 years, p<0.0001. Among multiple ovarian cancer cell lines, RMUG-S-ip2 mucinous ovarian cancer cells showed the highest src kinase activity. Moreover, oxaliplatin treatment induced phosphorylation of src kinase. This induced activity by oxaliplatin therapy was inhibited by concurrent administration of dasatinib. Targeting src with dasatinib *in vivo* showed significant anti-tumor effects in the RMUG-S-ip2 model, but not in the serous ovarian carcinoma (SKOV3-TR) model. Combination therapy of oxaliplatin with dasatinib further demonstrated significant effects on reducing cell viability, increasing apoptosis, and *in vivo* anti-tumor effects in the RMUG-S-ip2 model.

CONCLUSIONS—Our results suggest that poor survival of women with mucinous ovarian carcinoma is associated with resistance to cytotoxic therapy. Targeting src kinase with combination of dasatinib and oxaliplatin may be an attractive approach in this disease.

Keywords

ovarian cancer; mucinous; oxaliplatin; dasatinib; src kinase

INTRODUCTION

In 2010, over 21,000 women in the United States were diagnosed with ovarian carcinoma and almost 14,000 died from this disease, which ranks as the most common cause of death among gynecologic malignancies (1). The majority of ovarian carcinomas are of serous histology. Mucinous histology is relatively rare, accounting for 2–10% of all subtypes of epithelial ovarian carcinomas (2–3). Due to its relatively rare incidence, mucinous ovarian carcinomas are under-studied, but are thought to have poorer response to taxane and platinum chemotherapy, resulting in poor survival outcomes compared to serous ovarian carcinomas (4–7). Therefore, understanding the mechanisms contributing to mucinous ovarian cancer development and progression as well as novel therapeutic approaches are urgently needed.

Recent evidence suggests that mucinous ovarian carcinoma is histologically and molecularly similar to colorectal carcinomas, and has a distinct clinical pattern compared to other subtypes of ovarian carcinomas (8–9). The majority of colorectal carcinomas are of mucinous histology and patients with advanced-stage colorectal carcinoma are treated with chemotherapy containing oxaliplatin, a third generation platinum compound (10). Despite proven efficacy, resistance to oxaliplatin is a rising issue (11). Among proposed mechanisms, src kinase has been shown to play an important role in oxaliplatin resistance in colorectal, and pancreatic carcinomas (12–13). Src kinase is a non-receptor tyrosine kinase that regulates various aspects of tumor progression *via* multiple signaling pathways including cell survival (AKT), growth (Ras/MEK/ERK), metastasis (FAK/Paxillin/c-Jun), and angiogenesis (STAT3/VEGF) (14). Src kinase is known to be overexpressed in colorectal, pancreatic, lung, breast, and prostate carcinomas (15), and is thought to

contribute to chemotherapy resistance (13). In serous ovarian carcinoma, src kinase was reported to be overexpressed in advanced-stage disease (16). However, the role of src kinase in mucinous ovarian carcinoma is not known and was examined in the current study.

Here, we demonstrate that *(i)* advanced-stage mucinous ovarian carcinoma was associated with shorter survival time after progression or recurrence of disease compared to serous histology in a large cohort study, *(ii)* src kinase is highly activated among mucinous ovarian carcinomas, and *(iii)* targeting src kinase with combination of oxaliplatin and dasatinib demonstrated synergistic anti-tumor effects in mucinous ovarian cancer models.

MATERIALS AND METHODS

Clinical data

1302 ovarian cancer patients from cancer centers in the US and Japan were evaluated; 122 mucinous carcinoma patients (4th common, 9.3 ± 0.8%) were compared to 698 serous carcinoma patients (most common, 53.4 ± 1.4%) for survival. Patient age, preoperative CA125 value, histological subtypes, FIGO stage, grade, and cytoreduction were evaluated to determine potential impact on survival. Early- and advanced-stage disease was defined as FIGO state I/II and III/IV, respectively. Appendectomy is generally performed as a standard surgical procedure for mucinous ovarian carcinoma in the participating institutions. Gynecologic pathologists at each institution reviewed all of the specimens for assessing histology. Institutional Review Board approval was obtained at each institution.

Cell lines and cultures

RMUG-S and RMUG-L were cultured in RPMI-1640 media, supplemented with 10% fetal bovine serum and 0.1% gentamicin at 37°C in 5% CO_2 with 95% air. These cell lines were originally isolated from women with mucinous ovarian carcinoma (17). Ovarian serous carcinoma cell lines (HeyA8, HeyA8-MDR, SKOV3-ip1, and SKOV3-TR), clear cell carcinoma cell lines (ES-2 and RMG-2), and undifferentiated carcinoma cell lines (A2780 and A2780-CP20) were cultured in RPMI-1640 media supplemented with 15% fetal bovine serum and 0.1% gentamicin at 37°C in 5% CO_2 with 95% air. *In vitro* experiments were conducted with 80% cell confluence. All the cell lines were purchasedfrom American Type Culture Collection (ATCC, Manassas, VA) or Japanese Collection of Research Bioresources (JCRB, Tokyo, Japan).

Drugs and reagents

Anti-src (#2108) and anti-phospho src (Tyr419, #2101) antibodies for Western blot were purchased from Cell Signaling Technology, MA. Anti-phospho src antibody (Tyr419, AF2685) for immunohistochemistry staining was purchased from R&D Systems. Anti-CD31 (#53370) and anti-Ki67 (CP2498) antibodies were purchased from BD Pharmingen, CA and BioCare Medical, CA, respectively. Anti-vinculin (V9131) and antibeta-actin (A5316) antibodies were purchased from Sigma-Aldrich, MO. Oxaliplatin (Wyeth, NJ) was purchased from the institutional pharmacy. Dasatinib (Bristol-Myers Squibb, NY) was prepared as 20 mmol/L stock solution in DMSO. Paclitaxel, cisplatin, carboplatin,

doxorubicin, and topotecan was purchased from Sigma-Aldrich, MO. Etoposide was purchased from EMD4 Biosciences, NJ.

Microarray analysis

Gene expression was compared between mucinous (RMUG-S and L) and serous (SKOV3, OVCA3, 420, 429, 432, and 433) ovarian cancer cell lines. Pathway analysis was used to assess significant genes in mucinous compared to serous ovarian carcinoma (Ingenuity Pathway Analysis, version 7.5 (18), chip platform human genome U133 plus 2.0 array). Using the cutoff value of ±1.5-fold change, significant gene network was plotted (both direct and indirect relationship). Src kinase specific pathway analysis was performed and was shown as functional gene network ontology. Extraction of networks of molecular interactions for each dataset was performed using NetWalk, a random walk-based network retrieval algorithm (19), NetWalk-mediated analyses and visualizations were performed using NetWalker, an integrated platform for network based data analyses and visualization.

Apoptosis assay

For evaluation of apoptosis, PE Annexin V Apoptosis Detection Kit I (BD Pharmingen, CA) was used as described previously (20). Briefly, 5×10^5 RMUG-S-ip2 cells with serum containing medium were plated in 10 cm plates and incubated for 24 hours. Then, the media was replaced with fresh serum free medium. Treatment was started with control, oxaliplatin, dasatinib, and oxaliplatin with dasatinib for time periods ranging from 24 – 96 hours. Cell morphology was assessed by phase-contrast microscopy. Then, cells were removed from plate by trypsin-EDTA, washed twice with PBS, and resuspended with binding buffer at 10^6 cells/mL. FITC Annexin V and propidium iodide were added (each at 5 μL per 10^5 cells). Cells were incubated for 15 min at room temperature in the dark. Percentage of apoptosis was analysis with an EPICS XL flow cytometer (Beckman-Coulter, FL). Each sample was analyzed in triplicate.

Cytotoxicity assays

Cytotoxicity of oxaliplatin, dasatinib, and oxaliplatin with dasatinib treatment for RMUGS-ip2 was assessed with 3-(4,5-dimethylthiazol-2-yl)-2,5-diphenyltetrazolium bromide (MTT) uptake assay (Sigma-Aldrich, MO) as described previously (20). Briefly, 2×10^3 RMUG-S-ip1 or SKOV3-TR cells with serum containing medium were plated in each well of a 96-well plate and incubated for 24 hours. Then, the media was replaced with fresh serum free medium containing various concentrations of drugs (200 μL). Treatment was stopped at 48, 72, and 96-hour time points, and 0.15% MTT (50 μL) was added to each well. After a 2 hour incubation (37°C), medium was removed from each well and 100 μL of DMSO (Sigma-Aldrich, MO) was added. The absorbance at 570 nm wavelengths was measured by using a Falcon microplate reader (Becton Dickinson Labwave, NJ). Each sample was analyzed in triplicate. Isobologram analysis was performed to evaluate the cytotoxicity of oxaliplatin and dasatinib in RMUG-S-ip2 based on the dose-response cell-survival curves (21). Interaction index was calculated as described previously (22). Additive effect (equal to 1), synergistic effect (less than 1), and antagonistic effect (1 or greater) of the combination of oxaliplatin and dasatinib were determined based on the interaction index.

Cell cycle analysis

Proportions of cells in G1, S, and G2 phase were evaluated following treatment with either oxaliplatin, dasatinib, or oxaliplatin with dasatinib and compared to untreated controls. Briefly, 5×10^5 RMUG-S-ip2 cells with serum containing medium were plated in 10 cm dish plate and incubated 24 hours. Then, the media was replaced with fresh serum free medium. Treatment in each condition was stopped at 24, 48, 72, and 96- hour time points, and cells were removed from the plate by trypsin-EDTA, washed twice with PBS, and fixed with 70% ethanol (4°C overnight). Ethanol was removed and incubated with propidium iodine for 10 min. Cell cycle analysis was performed with an EPICS XL flow cytometer (Beckman-Coulter, FL). Each sample was analyzed in triplicate.

Western blot

Preparation of lysates from cultured cells was performed as previously described (23–24). Briefly, cells with 80% confluence were harvested and lysed in modified radioimmunoprecipitation (RIPA) assay buffer (50 mmol/L Tris, 150 mmol/L NaCl, 1% Triton X-100, 0.5% deoxycholate, 25 μg/mL leupeptin, 10 μg/mL aprotinin, 2 mmol/L EDTA, 1 mmol/L sodium orthovanadate) as described previously (24). Protein concentrations were measured with BCA Protein Assay Reagent Kit (Pierce, Biotechnology, IL), and 50 μg of lysate protein was mixed with SDS-PAGE on 10% gels transferred electrophoretically onto a nitrocellulose membrane. Non-fat milk powder (5%) in TBS-T [10 mmol/L Tris (pH 8), 150 mmol/L NaCl, 0.05% Tween 20] was used for protein block for 1 hour. The blots were incubated with anti-src (band at 60 kDa) and anti-phospho-src (60 kDa) antibodies at dilutions of 1:1000 for 4°C overnight, and washed with TBS-T. Antibody binding was probed by incubating the blots with horseradish peroxidase-conjugated goat anti-rabbit antibodies (GE Healthcare, WI) in 5% milk diluted with TBS-T for 1 hour at room temperature. Reactivity was visualized with enhanced chemiluminescence detection kit (Pierce Biotechnology, IL). Anti-vinculin (120 kDa) or anti-beta-actin (42 kDa) was used to evaluate an equal protein loading. Densitometry (ImageJ, NIH) was used to interpret the difference in the results of Western blot.

Immunohistochemistry

Immunohistochemical analysis for phospho-Src (Tyr419) and Src kinase was evaluated for human tissue samples embedded in paraffin blocks. For mouse tissues, phosphosrc, src kinase, and Ki67 were evaluated using formalin-fixed paraffin-embedded tumors. Optimal cutting temperature (OCT) compound-fixed tumor samples were used for CD31 staining. Briefly, the paraffin-embedded block was sectioned to 5 μm thickness, and deparaffinized (60°C overnight) and rehydrated. Antigen retrieval was done using Borg Decloaker (BioCare Medical, CA) with pressure cooker for anti-phospho-src and anti-src antibodies or Diva (BioCare Medical, CA) with steamer for anti-Ki67 antibody, respectively. For CD31 staining, sections were done on freshly cut frozen slides and these were fixed in cold acetone, and no antigen retrieval was necessary. Endogenous peroxidase and nonspecific epitopes were blocked with 3% H_2O_2 (Fisher Scientific, PA) in PBS for 12 minutes in room temperature, non-specific protein blinding was blocked with 5% normal horse serum and 1% normal goat serum for anti-Ki67 and anti-CD31 antibodies or 4% cold water fish skin

gelatin (Electron Microscopy Science, PA) for antiphospho-src or anti-src antibodies for 20 minutes in room temperature, respectively. Sections were incubated with primary antibodies at 4°C overnight. For negative control, sections were incubated without primary antibody and with human IgG antibody (Jackson Immunoresearch, PA). Goat anti-rabbit horseradish peroxidase-conjugated antibody (Jackson ImmunoResearch Laboratories, PA) for anti-CD31 and anti-Ki67 (1 hour, room temperature) or Mach 4 HR polymer (BioCare Medical, CA) for antiphospho- src and anti-src antibodies (20 minutes, room temperature) were used for secondary antibody, respectively. Signal was visualized after incubating with 3,3′-diaminobenzidine (Phoenix Biotechnologies, AL) and counterstaining with Gill's No. 3 hematoxylin (Sigma-Aldrich, MO).

Animal care

Nude mice (8–12 week old) were purchased from the National Cancer Institute/Frederick Cancer Research and Development Center (athymic female, Ncr-*nu*). The mice were quarantined, housed, and maintained under specific pathogen-free environment in the animal facility that is approved by the American Association for Accreditation of Laboratory Animal Care in agreement with the current regulations and standards of United States Department of Agriculture, Department of Health and Human Service, and National Institute of Health. Approval of the study protocols was obtained and supervised by the Institutional Animal Care and Use Committee at the University of Texas M.D. Anderson Cancer Center.

In vivo therapeutic experiment

In vivo model of mucinous ovarian carcinoma (RMUG-S-ip2) was created for the experiment (Supplemental methods) and the characteristics are shown in Figure S1. RMUG-S-ip2 cells were injected into the peritoneal cavity of 40 orthotopic nude mice (4×10^6 cells/mouse). After randomization into 4 groups of 10 mice (control, oxaliplatin alone, dasatinib alone, and oxaliplatin with dasatinib), treatment was initiated at 4 weeks following injection. Oxaliplatin (5 mg/kg/mouse) was given i.p. twice weekly after being dissolved in 5% dextrose and diluted with HBSS (13). Dasatinib (15 mg/kg/day/mouse) was given orally every day after being solubilized in citrate/citric acid buffer. Control mice received HBSS intraperitoneally twice a week and citrate buffer orally every day. Mice were monitored on a daily basis and weighted weekly. After 8 weeks of treatment, the mice were sacrificed, and total body weight of mouse, tumor locations and weight, and number of tumor nodules were recorded. Tumor samples were fixed with 10% formalin and embedded in paraffin or with OCT compound in liquid nitrogen. A similar experiment was also conducted with 25% drug dose reduction for both oxaliplatin and dasatinib in the RMUG-S-ip2 model. In addition, an experiment with the SKOV3-TR model (1.25×10^6 cells/mouse) was performed (mice were randomized into 4 groups as noted above and treatment was started 1 week after tumor cell injection and continued for 5 weeks).

Statistical analysis

Continuous variables were assessed for normal distribution (Kolmogorov-Smirnov test) and expressed as appropriate (mean with SD or median with range). Student's *t*-test or Mann-Whitney *U* test was performed to determine the statistical significance. Categorical variables were evaluated with Fisher's exact test (odds ratio and 95% confidence interval). For clinical

data analysis, to determine the significance of variables for the survival outcomes such as progression-free survival (PFS), overall survival (OS), and survival time after progression of disease or recurrence, univariate (Log rank test) and multivariate (Cox regression proportional hazard test) analyses were performed as appropriate. Survival curves were estimated with Kaplan-Meier method. *P*-values of less than 0.05 were considered as statistical significant (all, 2-tailed). The Statistical Package for Social Scientists software (SPSS, version 18.0, IL) was used for all analyses.

RESULTS

Mucinous ovarian carcinomas have distinct clinical characteristics

We first examined the clinical features of mucinous ovarian carcinoma compared to serous subtypes. The average age of women diagnosed with mucinous carcinoma was significantly younger than those with serous carcinoma (mean age, 54.1 ±14.8 *versus* 59.9 ±11.3, p=0.005). Distribution of FIGO stages among women with mucinous carcinomas was also significantly different from those with serous histology; majority of mucinous cases were early-stage while majority of serous cases were advanced-stage (p<0.0001, Figure 1A). CA-125 is a common biomarker for ovarian cancer utilized for diagnosis or follow-up after therapy. In women with mucinous ovarian carcinomas, CA- 125 was infrequently elevated compared to those with serous carcinoma (proportion of elevated CA-125 >35 IU/L in all stage cases, 66.7 *versus* 96.0%, odds ratio 0.56, 95%CI 0.38–0.83, p<0.0001, Figure 1B). Same results were noted in advanced stage (78.6 *versus* 97.4%, odds ratio 0.1, 95%CI 0.02–0.43, p=0.009). Among cases with elevated CA-125 (>35 IU/L), mucinous carcinoma patients showed lower CA-125 values compared to those with serous carcinoma (median 229 *versus* 475 IU/L, p<0.0001, Figure 1B). In multivariate analysis adjusted for other significant variables such as age, cytoreduction, and stage, mucinous histology remained an independent risk factor for survival of ovarian cancer patients (OS, p=0.045; and survival time after recurrence, p<0.0001). In early-stage disease, mucinous carcinoma patients showed better survival outcomes compared to those with serous carcinoma (10-year PFS, 78.7% *versus* 66.6%, p=0.039; 10-year OS, 89.5 *versus* 53.6%, p=0.086, Figure 1C). This difference likely represents the lower frequency of recurrence in women with early-stage mucinous ovarian carcinoma compared to those with serous histology (12.5 *versus* 30%, odds ratio 0.33, 95%CI 0.15–0.76, p=0.009). In advanced-stage disease, representing 36.9% of mucinous ovarian carcinoma cases, while there was no statistically significant difference in progression-free survival between mucinous and serous carcinoma patients (p=0.92), overall survival of mucinous carcinoma patients was significantly shorter than those with serous carcinoma (median OS, 1.67 *versus* 3.41 years, p=0.002, multivariate analysis). Similarly, survival time after progression of disease or recurrence after primary cytoreductive surgery was significantly shorter for women with mucinous carcinoma compared to those serous histology (median survival time, 0.53 *versus* 1.66 years, p<0.0001, multivariate analysis).

Gene expression and protein activity of src kinase in mucinous ovarian carcinomas

Given the poor clinical outcome of women with mucinous ovarian cancer, new therapeutic approaches are needed. In search of potentially useful targets, we next evaluated gene

expression in mucinous ovarian cancer cell lines (heat map shown in Figure S2). In pathway analysis, 41,329 genes were identified and 12,568 genes were functional and eligible for the analysis. The top 5 functional networks and 10 significant genes in mucinous ovarian carcinomas, when compared to serous ovarian carcinomas, are shown in Table S1 and Figure S3A–E, respectively. Src kinase was included in the top 3 networks for amino acid, molecular transport, and small molecular biochemistry although src mRNA was not differentially expressed between mucinous cell lines and serous cell lines (Figure S3C). These data suggest that regulation of src would be at the protein level. Thus, we examined the phosphorylation status of src in 12 ovarian cancer lines and 10 clinical mucinous ovarian cancer samples. Because src kinase activity is proposed as an important mechanism of resistance to chemotherapy (13), src kinase specific pathway analysis was performed for mucinous compared to serous ovarian carcinoma cell lines (Figure 2A). Among up-regulated genes associated with src kinase, 3 out of 12 genes were cadherin and catenin family members (CDH1, CDH5, and JUP; Table S2). Since increased expression of E-cadherin is a characteristic molecular feature of mucinous ovarian carcinoma (25), the increased activity of cadherin/catenin pathway in mucinous ovarian carcinoma may be associated with decreased src expression in mucinous ovarian carcinoma. There were some down-regulated genes associated with cell growth, adhesion, and motility in the mucinous ovarian cancer cells (ASAP1, ITGB3, RAC2, DNM1, and MYLK; Table S2).

Next, protein expression of src kinase was evaluated in 12 ovarian cancer cell lines and 2 non-transformed cell lines. The results were similar to the microarray analysis, and the level of total src expression in mucinous ovarian carcinoma cell line (RMUG-S-ip2) was the lowest among tested cell lines (Figure 2B). However, RMUG-S-ip2 showed the highest activity of src kinase, as determined by the ratio between phospho-src kinase divided by src kinase. Expression of src kinase (total src and phospho-src (Tyr419) was also evaluated in 10 mucinous ovarian cancer samples (Figure 2C). P-Src_{Y419} was localized in the cytoplasm of cancer cells, and all samples showed overexpression of src kinase.

Mucinous ovarian carcinomas are drug resistant

On the basis of clinical findings suggesting relative drug resistance, we next examined the sensitivity of mucinous (RMUG-S and L) and serous (SKOV3) ovarian cancer cell lines to various chemotherapeutic agents (Figure 2D). Compared to serous cell lines, mucinous carcinoma cell lines had significantly higher IC_{50} values for all tested chemotherapeutic agents. IC_{50} doses for oxaliplatin in RMUG-S-ip2 and RMUG-L-ip2 cells were 15.6 and 16.4 μg/mL, respectively (Figure S4). These values are comparable to colorectal cancer cell lines reported previously (2.8 to 29 μg/mL) (26–27). IC_{50} level of oxaliplatin in drug resistant cell line SKOV3-TR cells was 5.2 μg/mL (Figure S4).

Oxaliplatin-induced src kinase activity is inhibited by dasatinib

Next, we examined the effects of oxaliplatin on src expression and activation in the RMUG-S-ip2 and SKOV3-TR cells. Oxaliplatin induced src phosphorylation, but had no effect on total src levels in the RMUG-S-ip2 cells (Figure 3A). Oxaliplatin did not affect src phosphorylation in the SKOV3-TR cells (Figure S5). Treatment with dasatinib downregulated the phosphorylation of src kinase in the RMUG-S-ip2 cells (Figure 3B). We

then examined the effect of combination of oxaliplatin and dasatinib on src activation in RMUG-S-ip2 cells. In combination treatment, dasatinib blocked the oxaliplatin-induced increase in src activity (Figure 3B).

We next examined the effect of dasatinib on cell viability in the RMUG-S-ip2 and SKOV3-TR cells. RMUG-S-ip2 cells showed dose-dependent decrease in cell viability with dasatinib (Figure 4A). Conversely, SKOV3-TR cells did not show changes in viability with dasatinib (Figure 4B). RMUG-S-ip2 cells were then treated with various concentrations of oxaliplatin and dasatinib (Figure 4C). Oxaliplatin treatment alone affected cell viability of RMUG-S-ip2 cells (IC_{50}, 15.6 μg/mL), and adding dasatinib enhanced cytotoxic effects of oxaliplatin treatment. Isobologram analysis was performed, and the interaction index was <1 at all examined points, confirming the synergistic effects of oxaliplatin and dasatinib in cell viability (Figure 4D). Dasatinib concentration that showed a 50% reduction of oxaliplatin IC_{50} was 182 nM. In the SKOV3-TR cells, there was no difference in cell viability between oxaliplatin treatment alone and oxaliplatin with dasatinib (data not shown).

Effects of combination therapy with oxaliplatin and dasatinib were evaluated using apoptosis assays in RMUG-S-ip2 cells (Figure 4E and S6A). Monotherapy with either oxaliplatin or dasatinib significantly increased apoptosis compared to controls (proportion of apoptosis, control *versus* dasatinib *versus* oxaliplatin, 4.1±0.8 *versus* 8.5 ±0.3 *versus* 9.5 ±0.5%, both $p<0.01$). Combination therapy with oxaliplatin and dasatinib further enhanced the extent of apoptosis compared to monotherapy either with dasatinib or oxaliplatin (proportion of apoptosis, combination therapy *versus* dasatinib *versus* oxaliplatin, 26.8 ±0.3 *versus* 8.5 ±0.3 *versus* 9.5 ±0.5%, both $p<0.01$). These significant effects were observed at all time points examined (24 to 96 hours), and the effects were maximal at the 96 hour time point. Effects of therapy on cell cycle were also analyzed in the RMUG-S-ip2 cells (Figure 4F and S6B). Oxaliplatin significantly increased the proportion of cells in S phase and decreased both G1 and G2 phase compared to control ($p<0.001$). Dasatinib treatment did not affect cell cycle distribution. The results of combination of oxaliplatin and dasatinib remained similar to the results of oxaliplatin treatment ($p<0.001$ compared to control).

In vivo anti-tumor effects of oxaliplatin and dasatinib in ovarian carcinoma

Next, an *in vivo* experiment was performed to evaluate the anti-tumor effects of combination therapy with oxaliplatin and dasatinib. Compared to the control group, monotherapy with oxaliplatin or dasatinib resulted in significantly smaller tumor weight (tumor weight reduction, control *versus* oxaliplatin, 58.6%, $p<0.01$; and control *versus* dasatinib 65.8%, $p<0.01$) and number of tumor nodules (tumor nodule reduction, control *versus* oxaliplatin, 45.9%, $p<0.05$; and control *versus* dasatinib 53.6%, $p<0.05$, Figure 5A). Combination therapy with oxaliplatin and dasatinib further showed significant antitumor effects compared to either monotherapy: reduction of tumor weight, oxaliplatin *versus* combination, 79.1%, $p<0.01$; and dasatinib *versus* combination, 74.7%, $p<0.01$, respectively (Figure 5A). Compared to controls, combination therapy resulted in 91.3% tumor weight reduction and 77.4% decrease in tumor nodule number, respectively (both $p<0.01$). There were 4 out of 10 mice with metastasis to liver parenchyma in the control group, but none in the treatment groups. Mice treated with dasatinib did not have any differences in body weight compared to

the control group (data not shown). To evaluate if there may be synergistic anti-tumor activity with oxaliplatin and dasatinib, we conducted an *in vivo* experiment using RMUG-S-ip2 with 25% dose reduction of oxaliplatin and dasatinib (Figure S7). The results of anti-tumor effects in lower dose oxaliplatin and dasatinib were similar to the results of original experiment: anti-tumor effects of oxaliplatin alone, dasatinib alone, and combination of oxaliplatin and dasatinib were 65.4%, 60.3%, and 88.8%, respectively, when compared to the control group (all $p<0.05$). These results suggest possible synergistic anti-tumor effects of oxaliplatin and dasatinib in mucinous ovarian carcinoma.

In contrast to mucinous ovarian carcinoma, serous ovarian carcinoma showed different anti-tumor effects with dasatinib treatment (Figure 5A). While RMUG-S-ip2 showed significant anti-tumor effects with dasatinib monotherapy, there were no significant antitumor effects in the SKOV3-TR model (mean tumor weight, dasatinib *versus* control, 1.09 ±0.29 *versus* 1.42 ±0.29, p=0.42). These *in vivo* effects with dasatinib monotherapy corresponded well with the effects noted in the *in vitro* experiments with the mucinous and serous cancer cell lines (Figure 4A–B). Oxaliplatin alone showed significant anti-tumor effects in the SKOV3-TR model when compared to control (mean tumor weight, oxaliplatin *versus* control, 0.48 ±0.12 *versus* 1.42 ±0.29, p=0.01), and the extent of tumor reduction rate with oxaliplatin therapy was similar to the RUMG-S-ip2 model (58.6% and 65.9%, respectively). Immunohistochemical staining was performed on the RMUG-S-ip2 tumor tissues obtained from the *in vivo* experiments to assess effects on proliferation and microvessel density (Figure 5B). Tumors obtained from the dasatinib treatment group showed substantially decreased p-Src_{Y419} expression compared to the control group. In tumors obtained from the oxaliplatin treatment group, there were areas that showed focally increased expression of p-Src_{Y419}. This was not seen in tumors treated with oxaliplatin and dasatinib. This induction of activated src following oxaliplatin treatment supports the *in vitro* findings. Numbers of positive Ki67 cells as well as microvessel density were significantly decreased in the combination therapy group compared to monotherapy group (all $p<0.05$, Figure 5B).

DISCUSSION

Our clinical, *in vitro*, and *in vivo* results highlight important features that contribute to the distinct mechanisms of mucinous ovarian carcinoma pathogenesis. Targeting src kinase with dasatinib inhibited oxaliplatin-induced src kinase activity and showed synergistic anti-tumor effects in a mucinous ovarian carcinoma model. Several key areas in this notable observation deserve special mention.

Mucinous ovarian carcinoma is known to be associated with poorer patient outcome compared to other subtypes of ovarian carcinoma (4, 7–8). Our results not only support previous studies, but also imply that mucinous ovarian carcinomas are associated with slow progression and chemoresistance that may partly be explained by the hypothesis that mucinous ovarian carcinomas are genetically stable (28). To explain the distinct clinical characteristics of mucinous ovarian carcinomas, there are several molecular characteristics that can distinguish these tumors from serous carcinomas (8). Well studied biomarkers of mucinous ovarian carcinomas include cadherin, matrix metalloproteinases, WT-1, CA125 and CEA. In gene expression analyses with microarrays, the profile patterns among these

two cell lines were distinctly different (8). While mucinous ovarian carcinomas are less likely to have BRCA or p53 mutations, Kras mutations are seen with greater frequency compared to serous carcinomas (8). Kras mutation, reported in nearly 40%, is also common in colorectal carcinoma (29). These molecular characteristics further support the premise that mucinous ovarian carcinoma is not only distinct from serous ovarian carcinomas, but histologically and molecularly mimics colorectal carcinoma (8).

Oxaliplatin has been used for ovarian carcinomas in various clinical trials and has shown a wide range of anti-tumor activity (20–75%) (12, 30). Induction of src kinase activity *via* ROS produced during the process of oxaliplatin-DNA adduct formation has been proposed as one of mechanisms associated with oxaliplatin resistance in colorectal carcinoma (13). Thus, dasatinib holds potential for enhancing the efficacy of oxaliplatin chemotherapy (31). In our study, similar findings were observed in mucinous ovarian carcinoma and treatment with oxaliplatin induced activation of src kinase in RMUG-S-ip2 cells. Similar induction was not observed in serous ovarian cancer cells. Induction of src kinase activity may be associated with drug resistance *via* AKT and Ras pathways in mucinous ovarian carcinoma (13, 32–33). However, it is not completely clear how src kinase activity is induced in mucinous ovarian carcinoma, but not in serous cancer cells. To date, the mechanism of ROS-induced src activation is not fully understood (13). As demonstrated in colorectal carcinoma models, pretreatment with an anti-oxidant agent such as a vitamin E analogue, inhibited phosphorylation of src kinase (13). Thus, it is possible that cell innate anti-oxidative functions such as superoxide dismutase in mucinous ovarian carcinoma may be different from serous carcinoma (13).

Mucinous ovarian carcinomas showed not only induction of src kinase activity with oxaliplatin treatment, but also increased activity of src kinase in non-stress conditions. However, expression of src kinase at mRNA and protein level in RMUG-S-ip2 cells was lower compared to serous cancer cell lines. This suggests that there is a mechanism that contributes to the activation of src kinase at the protein level, but not necessarily at the gene expression level. Theoretically, increased upstream signaling, phosphatase activity, and protein-protein interactions downstream of src could be the mechanisms that explain increased activity of src kinase. To date, there is little evidence regarding mutation of src kinase (14–15). While phosphorylation of Y419 tyrosine residue activates src kinase, phosphorylation of Y530 tyrosine residue inactivates src kinase (15). It is possible that the RMUG-S-ip2 cells may have increased phosphatase activity that dephosphorylates Y530. For protein-protein interaction as the mechanism of src kinase activation, there are several binding partners of src kinase that can regulate its catalytic activity including the p130cas/paxillin complex (34). Role of 130cas/paxillin in mucinous ovarian carcinomas is yet to be elucidated and needs further investigation. Because RMUG-S-ip2 cells showed highest src activity while SKOV3-TR showed minimum src activity, baseline activity of src kinase may be a predictor of response to dasatinib therapy.

In summary, mucinous ovarian carcinoma has distinct characteristics from serous carcinoma. In light of results presented here, combination therapy with oxaliplatin and dasatinib is an attractive approach for further clinical development.

Acknowledgments

Grant support: the NIH (CA 110793, 109298, P50 CA083639, P50 CA098258, CA128797, RC2GM092599), the Ovarian Cancer Research Fund, Inc. (Program Project Development Grant), the DOD (OC073399, OC093146, BC085265), the Zarrow Foundation, the Marcus Foundation, and the Betty Anne Asche Murray Distinguished Professorship, and NCI institutional Core Grant CA16672; NCI-DHHS-NIH T32 Training Grant (T32 CA101642) (JNB, RLS); GCF/Gail MacNeil KOH Research Grant (RLS); Meyer and Ida Gordon Foundation #2 (KM); and GCF/OCRF Ann Schreiber Ovarian Cancer Research Grant (KM).

References

1. Jemal A, Siegel R, Xu J, Ward E. Cancer statistics, 2010. CA Cancer J Clin. 2010 Sep-Oct;60(5): 277–300. [PubMed: 20610543]
2. Harrison ML, Jameson C, Gore ME. Mucinous ovarian cancer. Int J Gynecol Cancer. 2008 Mar-Apr;18(2):209–14. [PubMed: 17624989]
3. Matsuo K, Bond VK, Eno ML, Im DD, Rosenshein NB. Low drug resistance to both platinum and taxane chemotherapy on an in vitro drug resistance assay predicts improved survival in patients with advanced epithelial ovarian, fallopian and peritoneal cancer. Int J Cancer. 2009 Dec 1; 125(11): 2721–7. [PubMed: 19530239]
4. Hess V, Hern A'R, Nasiri N, King DM, Blake PR, Barton DP, Shepherd JH, Ind T, Bridges J, Harrington K, Kaye SB, Gore ME. Mucinous epithelial ovarian cancer: a separate entity requiring specific treatment. J Clin Oncol. 2004 Mar 15; 22(6):1040–4. [PubMed: 15020606]
5. Winter WE 3rd, Maxwell GL, Tian C, Carlson JW, Ozols RF, Rose PG, Markman M, Armstrong DK, Muggia F, McGuire WP. Prognostic factors for stage III epithelial ovarian cancer: a Gynecologic Oncology Group Study. J Clin Oncol. 2007 Aug 20; 25(24):3621–7. [PubMed: 17704411]
6. Bamias A, Psaltopoulou T, Sotiropoulou M, Haidopoulos D, Lianos E, Bournakis E, Papadimitriou C, Rodolakis A, Vlahos G, Dimopoulos MA. Mucinous but not clear cell histology is associated with inferior survival in patients with advanced stage ovarian carcinoma treated with platinum-paclitaxel chemotherapy. Cancer. 2010 Mar 15; 116(6):1462–8. [PubMed: 20108307]
7. Shimada M, Kigawa J, Ohishi Y, Yasuda M, Suzuki M, Hiura M, Nishimura R, Tabata T, Sugiyama T, Kaku T. Clinicopathological characteristics of mucinous adenocarcinoma of the ovary. Gynecol Oncol. 2009 Jun; 113(3):331–4. [PubMed: 19275957]
8. Frumovitz M, Schmeler KM, Malpica A, Sood AK, Gershenson DM. Unmasking the complexities of mucinous ovarian carcinoma. Gynecol Oncol. 2010 Jun; 117(3):491–6. [PubMed: 20332054]
9. Gomez-Raposo C, Mendiola M, Barriuso J, Hardisson D, Redondo A. Molecular characterization of ovarian cancer by gene-expression profiling. Gynecol Oncol. 2010 Jul; 118(1):88–92. [PubMed: 20439111]
10. Cunningham D, Atkin W, Lenz HJ, Lynch HT, Minsky B, Nordlinger B, Starling N. Colorectal cancer. Lancet. 2010 Mar 20; 375(9719):1030–47. [PubMed: 20304247]
11. Almendro V, Ametller E, Garcia-Recio S, Collazo O, Casas I, Auge JM, Maurel J, Gascon P. The role of MMP7 and its cross-talk with the FAS/FASL system during the acquisition of chemoresistance to oxaliplatin. PLoS One. 2009; 4(3):e4728. [PubMed: 19266094]
12. Fu S, Kavanagh JJ, Hu W, Bast RC Jr. Clinical application of oxaliplatin in epithelial ovarian cancer. Int J Gynecol Cancer. 2006 Sep-Oct;16(5):1717–32. [PubMed: 17009963]
13. Kopetz S, Lesslie DP, Dallas NA, Park SI, Johnson M, Parikh NU, Kim MP, Abbruzzese JL, Ellis LM, Chandra J, Gallick GE. Synergistic activity of the SRC family kinase inhibitor dasatinib and oxaliplatin in colon carcinoma cells is mediated by oxidative stress. Cancer Res. 2009 May 1; 69(9):3842–9. [PubMed: 19383922]
14. Summy JM, Gallick GE. Treatment for advanced tumors: SRC reclaims center stage. Clin Cancer Res. 2006 Mar 1; 12(5):1398–401. [PubMed: 16533761]
15. Kim LC, Song L, Haura EB. Src kinases as therapeutic targets for cancer. Nat Rev Clin Oncol. 2009 Oct; 6(10):587–95. [PubMed: 19787002]

16. Wiener JR, Windham TC, Estrella VC, Parikh NU, Thall PF, Deavers MT, Bast RC, Mills GB, Gallick GE. Activated SRC protein tyrosine kinase is overexpressed in late-stage human ovarian cancers. Gynecol Oncol. 2003 Jan; 88(1):73–9. [PubMed: 12504632]

17. Sakayori M, Nozawa S, Udagawa Y, Chin K, Lee SG, Sakuma T, Iizuka R, Wada Y, Yoshida S, Takeda Y. Biological properties of two newly established cell lines (RMUG-S, RMUG-L) from a human ovarian mucinous cystadenocarcinoma. Hum Cell. 1990 Mar; 3(1):52–6. [PubMed: 2083224]

18. Ingenuity Systems, Inc. (http://www.ingenuity.com)

19. Komurov K, Padron D, Cheng T, Roth M, Rosenblatt KP, White MA. Comprehensive mapping of the human kinome to epidermal growth factor receptor signaling. J Biol Chem. 2010 Jul 2; 285(27):21134–42. [PubMed: 20421302]

20. Lee JW, Han HD, Shahzad MM, Kim SW, Mangala LS, Nick AM, Lu C, Langley RR, Schmandt R, Kim HS, Mao S, Gooya J, Fazenbaker C, Jackson D, Tice DA, Landen CN, Coleman RL, Sood AK. EphA2 immunoconjugate as molecularly targeted chemotherapy for ovarian carcinoma. J Natl Cancer Inst. 2009 Sep 2; 101(17):1193–205. [PubMed: 19641174]

21. Machado SG, Robinson GA. A direct, general approach based on isobolograms for assessing the joint action of drugs in pre-clinical experiments. Stat Med. 1994 Nov 30; 13(22):2289–309. [PubMed: 7855464]

22. Lu G, Xiao H, You H, Lin Y, Jin H, Snagaski B, Yang CS. Synergistic inhibition of lung tumorigenesis by a combination of green tea polyphenols and atorvastatin. Clin Cancer Res. 2008 Aug 1; 14(15):4981–8. [PubMed: 18676773]

23. Halder J, Kamat AA, Landen CN Jr, Han LY, Lutgendorf SK, Lin YG, Merritt WM, Jennings NB, Chavez-Reyes A, Coleman RL, Gershenson DM, Schmandt R, Cole SW, Lopez-Berestein G, Sood AK. Focal adhesion kinase targeting using in vivo short interfering RNA delivery in neutral liposomes for ovarian carcinoma therapy. Clin Cancer Res. 2006 Aug 15; 12(16):4916–24. [PubMed: 16914580]

24. Mangala LS, Zuzel V, Schmandt R, Leshane ES, Halder JB, Armaiz-Pena GN, Spannuth WA, Tanaka T, Shahzad MM, Lin YG, Nick AM, Danes CG, Lee JW, Jennings NB, Vivas-Mejia PE, Wolf JK, Coleman RL, Siddik ZH, Lopez-Berestein G, Lutsenko S, Sood AK. Therapeutic Targeting of ATP7B in Ovarian Carcinoma. Clin Cancer Res. 2009 Jun 1; 15(11):3770–80. [PubMed: 19470734]

25. Sarrio D, Moreno-Bueno G, Sanchez-Estevez C, Banon-Rodriguez I, Hernandez-Cortes G, Hardisson D, Palacios J. Expression of cadherins and catenins correlates with distinct histologic types of ovarian carcinomas. Hum Pathol. 2006 Aug; 37(8):1042–9. [PubMed: 16867867]

26. Flis S, Splwinski J. Inhibitory effects of 5-fluorouracil and oxaliplatin on human colorectal cancer cell survival are synergistically enhanced by sulindac sulfide. Anticancer Res. 2009 Jan; 29(1): 435–41. [PubMed: 19331183]

27. Jiang H, Chen K, He J, Pan F, Li J, Chen J, Chen W, Liang H. Association of pregnane X receptor with multidrug resistance-related protein 3 and its role in human colon cancer chemoresistance. J Gastrointest Surg. 2009 Oct; 13(10):1831–8. [PubMed: 19593667]

28. Kurman RJ, Shih Ie M. The origin and pathogenesis of epithelial ovarian cancer: a proposed unifying theory. Am J Surg Pathol. 2010 Mar; 34(3):433–43. [PubMed: 20154587]

29. Cejas P, Lopez-Gomez M, Aguayo C, Madero R, de Castro Carpeno J, Belda-Iniesta C, Barriuso J, Moreno Garcia V, Larrauri J, Lopez R, Casado E, Gonzalez-Baron M, Feliu J. KRAS mutations in primary colorectal cancer tumors and related metastases: a potential role in prediction of lung metastasis. PLoS One. 2009; 4(12):e8199. [PubMed: 20020061]

30. Matsuo K, Lin YG, Roman LD, Sood AK. Overcoming platinum resistance in ovarian carcinoma. Expert Opin Investig Drugs. 2010 in-press.

31. Lieu C, Kopetz S. The SRC family of protein tyrosine kinases: a new and promising target for colorectal cancer therapy. Clin Colorectal Cancer. 2010 Apr; 9(2):89–94. [PubMed: 20378502]

32. Peterson-Roth E, Brdlik CM, Glazer PM. Src-Induced cisplatin resistance mediated by cell-to-cell communication. Cancer Res. 2009 Apr 15; 69(8):3619–24. [PubMed: 19351863]

33. Pengetnze Y, Steed M, Roby KF, Terranova PF, Taylor CC. Src tyrosine kinase promotes survival and resistance to chemotherapeutics in a mouse ovarian cancer cell line. Biochem Biophys Res Commun. 2003 Sep 19; 309(2):377–83. [PubMed: 12951060]

34. Schuh NR, Guerrero MS, Schrecengost RS, Bouton AH. BCAR3 regulates Src/p130 Cas association, Src kinase activity, and breast cancer adhesion signaling. J Biol Chem. 2010 Jan 22; 285(4):2309–17. [PubMed: 19940159]

Statement of Translational Relevance

Recent studies have shown that mucinous ovarian carcinomas have a distinct clinical pattern compared to other subtypes of ovarian carcinomas. The first part of our study demonstrated poorer survival outcome in mucinous ovarian carcinoma in comparison to serous ovarian cancer, the most common subtype of ovarian carcinoma, in a large sample size. Genomic approaches using mucinous ovarian cancer cell lines pointed to the Src kinase being involved in many of the activated pathways. In validation studies, Src was found to be highly activated in mucinous ovarian cancer. The mucinous ovarian cancer cells were resistant to most chemotherapy drugs. A Src inhibitor, dasatinib, inhibited oxaliplatin-induced src activation and enhanced anti-tumor effects of oxaliplatin in both *in vitro* and *in vivo* models of mucinous ovarian carcinoma. These findings implicate Src as a critical therapeutic target in mucinous ovarian carcinoma.

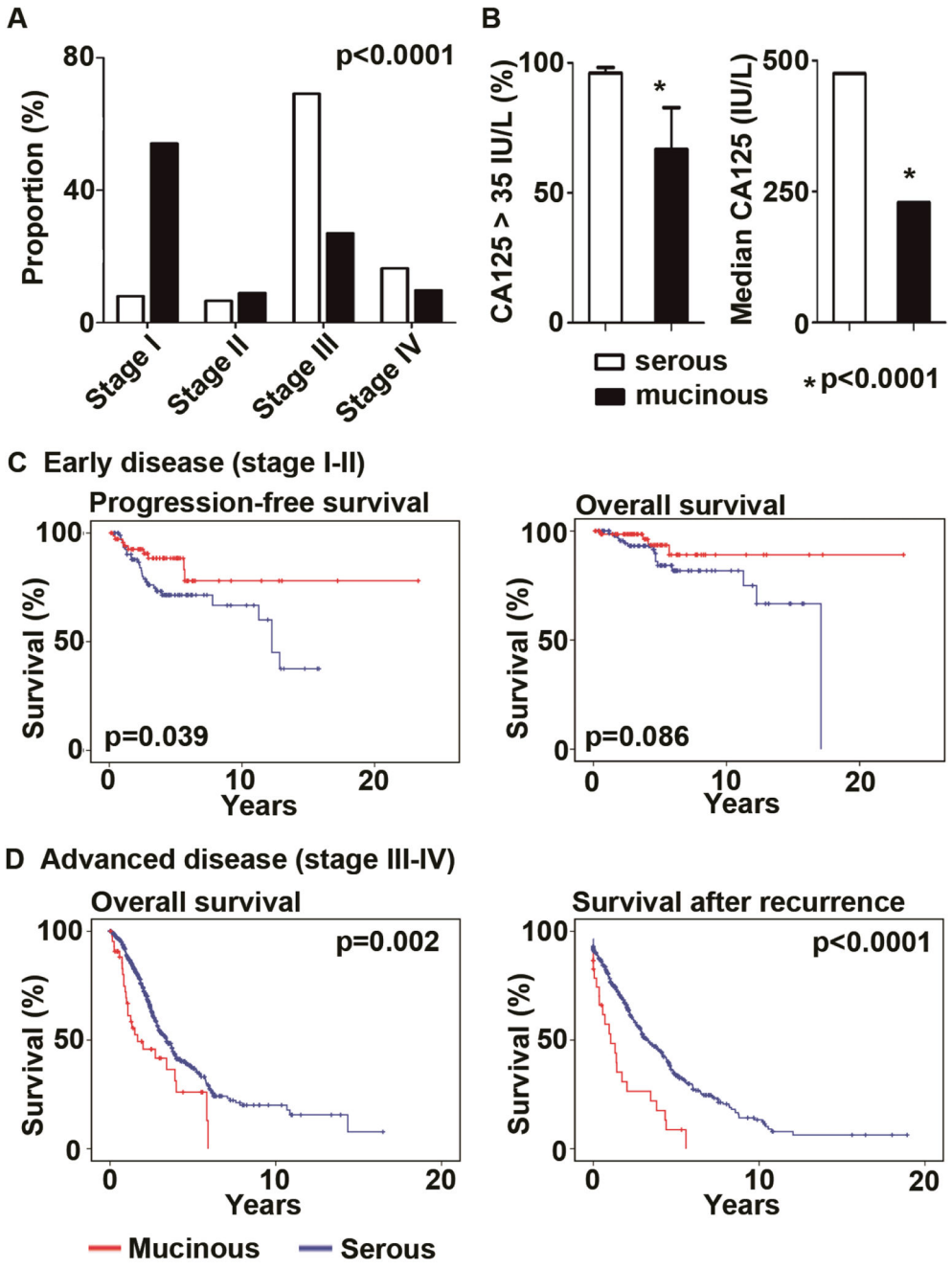

Figure 1. Clinical significance of mucinous ovarian carcinomas

(A) Proportion of FIGO stage in 122 mucinous (black bar) and 698 serous (white bar) carcinoma patients is shown. (B) Proportion of patients with elevated CA-125 (>35 IU/L) and median CA-125 value among patients with mucinous or serous carcinomas are shown. Bar for CA125 >35 IU/L represents frequency with 95%CI. (C) Kaplan-Meier survival curves for progression-free survival and overall survival in early-stage disease are shown. (D) Kaplan-Meier survival curves for overall survival and survival time after progression or recurrence of disease are shown.

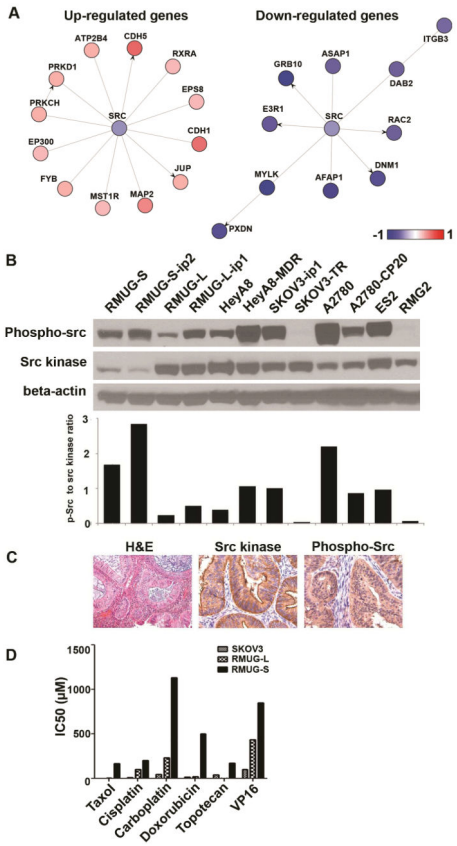

Figure 2. Expression and activity of Src kinase in mucinous ovarian carcinomas

(A) Src pathway specific analysis with gene network ontology is shown. Expressions of mucinous ovarian carcinoma cell lines were compared to ovarian serous carcinoma cell lines. (B) Western blot analysis for phospho-src (p-src) and src kinase in 14 cell lines is shown. Cells were incubated in serum containing media and collected in 70–80% confluence. (C) Immunohistochemistry staining for src kinase and phospho-src for human mucinous ovarian carcinomas are shown (magnification ×200). (D) Cell viability assay for 3 cell lines and 6 chemotherapeutic agents is shown.

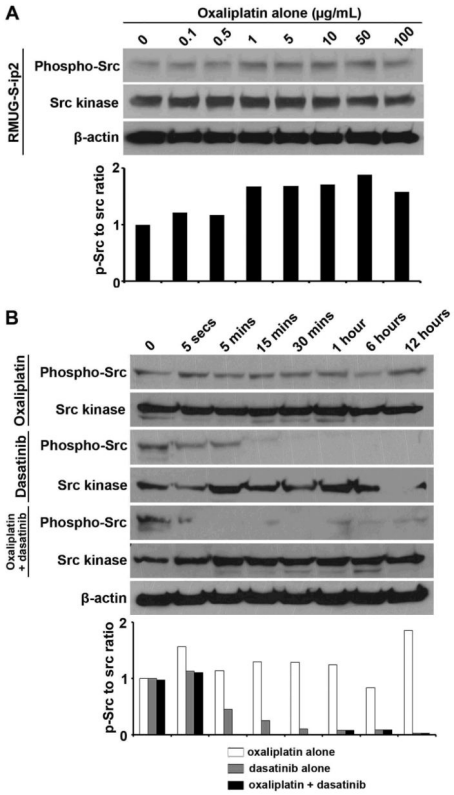

Figure 3. Modulation of src kinase activity with oxaliplatin and dasatinib

(A) Western blot analysis for phospho-src, src, phospho-AKT, and AKT is shown over time. RMUG-S-ip2 and SKOV3-TR were treated with IC_{50} dose of oxaliplatin (RMUG-S-ip2 15.6 μg/mL, and SKOV3-TR 5.2 μg/mL). (B, C) Western blot analysis for dose-kinetic study is shown for RMUG-S-ip2 treated with dasatinib alone (B) or dasatinib with oxaliplatin (C). The experiment time was stopped at 30 mins. IC_{50} dose of oxaliplatin (15.6 μg/mL) was used.

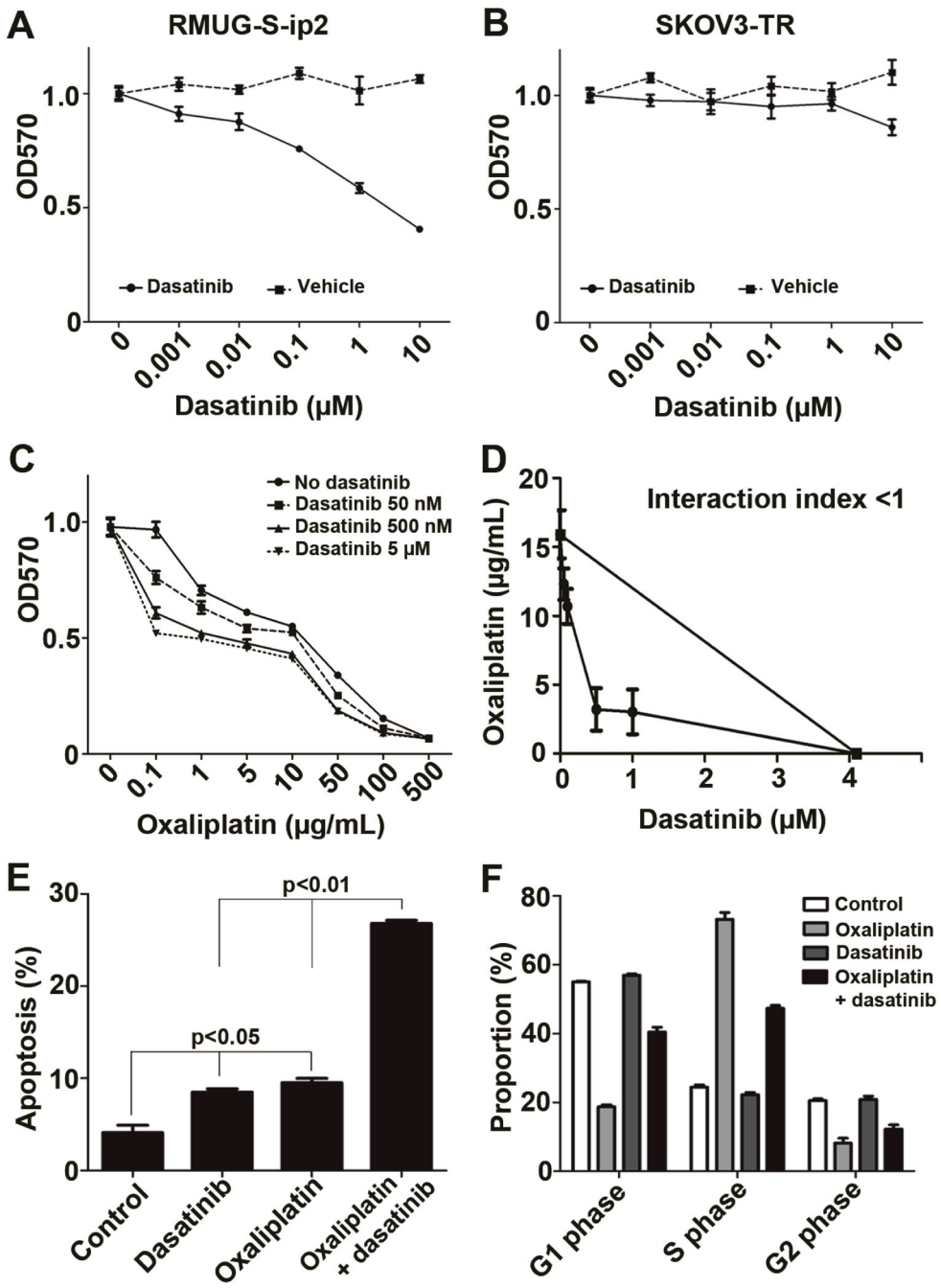

Figure 4. ***In vitro*** **effects of combination therapy with oxaliplatin and dasatinib in mucinous ovarian carcinoma**

(A and B) Cell viability assays for dasatinib treatment in RMUG-S-ip2 (A) and SKOV3-TR (B) are shown. IC_{50} dose of dasatinib in RMUG-S-ip2 was 3.1 μM. DMSO was used as drug vehicle. (C) Cell viability assay for combination of oxaliplatin and dasatinib in RMUG-S-ip2 is shown. Experimental time-point was 72 hours. (D) Isobologram analysis for oxaliplatin and dasatinib in RMUG-S-ip2 is shown. Interaction index was <1 at all examined points. Dasatinib concentration that reduced 50% of oxaliplatin IC_{50} dose was 182 nM. (E) Apoptosis assay for oxaliplatin and dasatinib is shown at the 96 hour time-point.

Chemotherapeutic doses used for the assay were oxaliplatin 15.6 μg/mL and dasatinib 182 nM, respectively. (F) Cell cycle analysis of RMUG-S-ip2 treated with oxaliplatin and dasatinib is shown. Dot represents mean with SE in Figure A to D. Bar represents mean with SE in Figure E and F.

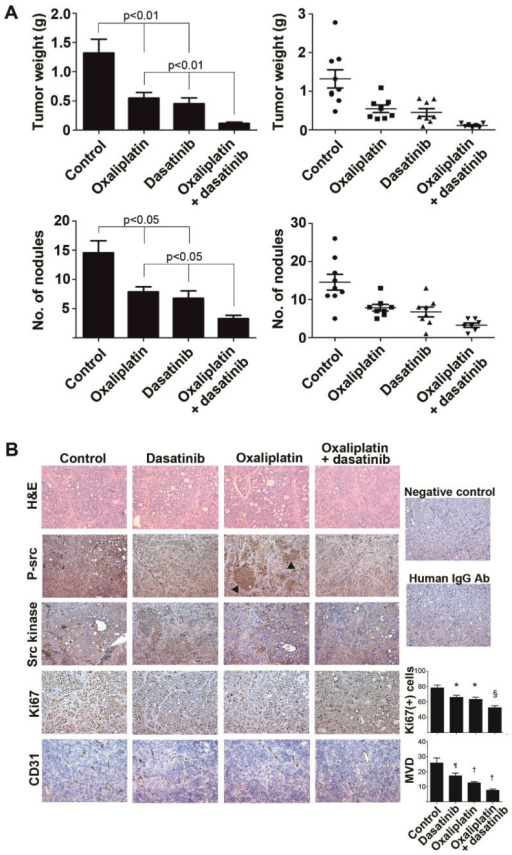

Figure 5. ***In vivo*** **anti-tumor effects of combination therapy with oxaliplatin and dasatinib in mucinous ovarian carcinoma**

(A) Tumor weight (upper figures) and number of nodules (lower figures) are shown for 4 groups. Treatment was started 4 weeks from RMUG-S-ip2 injection and continued for 8 weeks. Bar represents mean with SE. (B) Immunohistochemistry staining for phospho-src (p-src), src kinase, Ki67, CD31 is shown in 4 groups. Negative control: no primary antibody used, and human IgG Ab: human IgG antibody was used as primary antibody. Arrow head: focal increased expression of phospho-src in tumors treated with oxaliplatin. For Ki67 staining, * $p<0.01$, § $p<0.0001$, compared to control (number of positive Ki67 cells per ×100 field). For CD31 staining, ¶ $p<0.05$, † $p<0.01$, compared to control. MVD, microvessel density (number of microvessel per ×200 field).